Ehsan Daneshkhah
POLITECNICO DI TORINO
Department of Mechanical and Aerospace Engineering
C.so Duca degli Abruzzi, 24 - 10129 Torino, Italy
Tel. +39 349.743.0924
e-mail ehsan.daneshkhah@polito.it

Doctoral Thesis Revision

"Free vibration and post-buckling analyses of thin-walled beam and flexible plate structures through the Unified Formulation" by Ehsan Daneshkhah under the supervision of Professor Erasmo Carrera and Professor Alfonso Pagani.

Dear Professor Cinefra and Professor Bagassi,

We appreciate your efforts in handling, commenting, and giving us the possibility to revise the thesis. We would like to thank you all for pointing out the merit of our work and for recommending the award of the Ph.D. at Politecnico di Torino after pertinent revisions are made. We are profoundly grateful for the useful criticisms which helped us to improve the quality of our research work.

All the points raised by the Doctoral Examination Committee have been taken into account during the revision process of our work. The revised version of the thesis is enclosed to this letter along with a list of the main modifications made and a point-by-point reply letter to the Reviewer' criticisms.

Kind regards,

Ehsan Daneshkhah

Torino, Italy

September 8, 2022

Kind regards

List of the main modifications made during the revision work

- A section is added to Chapter 5 in order to provide some details of the implementation of von Mises constitutive model for elastoplastic material.
- Chapter 9 including the summary, conclusions, and future perspectives is added to the end of thesis.
- The tables of DOF for the comparison of ABQ and CUF models are provided for Chapters 3-6.
- For the sake of clarification, some explanations have been added to the results.
- The typos and mistakes have been corrected.

<u>Doctoral Examination Committee 1, Professor Cinefra:</u>

These thesis presents refined nonlinear structural theories for the free vibration and post-buckling response of thin-walled beam and flexible plate structures. In this regard, the Unified Formulation is employed to obtain nonlinear governing equations of the finite beam and plate elements. Then, various assessments are conducted related to the thin-walled beam and flexible plate structures. The free vibration response of thin-walled isotropic and composite beams is accurately evaluated, and the Vibration Correlation Technique is used in order to investigate the variations of natural frequencies in thin-walled laminated isotropic and composite beam structures under compression. The physically and geometrically nonlinear analysis of thin-walled beams is also investigated using Newton–Raphson linearization scheme with the path-following method based on the arc-length constraint. The large-deflection and post-buckling of isotropic and composite plates under axial, in-plane shear and combined loadings are analyzed considering different strain-displacement assumptions, and the corresponding equilibrium curves and stress distributions are presented. Furthermore, the effects of load and displacement boundary conditions in the post-buckled laminated composite plates are investigated, and the effects of stiffeners are assessed. The results show that the present method based on the Unified Formulation can be efficiently used for accurate structural analysis, including the free vibration and post-buckling of the thin-walled beam and flexible plate structures.

The manuscript is well written and organized. Some typos are highlighted in the attached pdf and some minor comments are provided in order to improve the clarity of the manuscript. Each part is clearly introduced and developed and test cases are properly selected and described. Figures and Tables are carefully generated and discussed. The Bibliography is rather complete and satisfactory. The general evaluation of the work is positive. Nevertheless, the reviewer asks to clarify the following point:

Comment 1.1

Chapter 4: how do you include the compressive load in the free-vibration analysis model?

Reply 1.1

The author thank the Reviewer for this concern. The compressive load results in the decrease of stiffness of the structure. This effect is considered by the calculation of geometric stiffness of the structure. In the presented method, this geometric stiffness contribution is considered for the applied loading, and then the free vibration analysis is conducted for the pre-stressed structure. The relevant explanation has been added in the first section of Chapter4:

In the case of small displacements and linear buckling, the tangent stiffness can be approximated as the sum of the linear stiffness ($\boldsymbol{K}_0$) and the geometric stiffness ($\boldsymbol{K}_\sigma$) contribution [115]:

$$\boldsymbol{K}_T \simeq \boldsymbol{K}_0 + \boldsymbol{K}_\sigma \tag{4.1}$$

Afterwards, by considering harmonic motion around quasi-static equilibrium states, the eigenvalues problem can be solved as follows:

$$(-\omega_k^2 \boldsymbol{M} + \boldsymbol{K}_T)\boldsymbol{u}_k = 0 \tag{4.2}$$

where ω_k are the natural frequencies, and $\boldsymbol{u}_k$ is the k th eigenvector.

Comment 1.2

Chapter 5: how does the candidate include the von Mises constitutive model for elasto-plastic material, as in Chapter 5, in the non-linear models presented in Chapter 2? One of the hypothesis declared is constant matrix C.

Reply 1.2

The author thank the Reviewer for pointing this out. According to the comment of the Reviewer, a section is added to Chapter 5 in order to provide some details of the implementation of model. In fact, for this chapter the C matrix is being updated consistently. The relevant section has been added to Chapter 5:

5.2 The von Mises model for elastoplasticity

In his section, the von Mises model implemented for the nonlinear framework of metallic elastoplastic materials is provided [42, 185]. Based on the isotropic work-hardening von Mises constitutive model, the stress-strain relation is given by:

$$\boldsymbol{\sigma} = \mathbf{C}^{cep} \boldsymbol{\varepsilon}^e \tag{5.1}$$

where $\boldsymbol{\varepsilon}^e$ is the elastic component of the strain tensor, and the consistent tangent elastoplastic operator $\mathbf{C}^{cep}$ is a fourth-order tensor that describes the elastoplastic nature of the material and relates the current values of stress and strain such that:

$$\mathbf{C}^{cep} = \frac{\partial \boldsymbol{\sigma}_{n+1}}{\partial \boldsymbol{\varepsilon}_{n+1}} \tag{5.2}$$

In the current implementation of the model, a piece-wise linear hardening can be prescribed by providing a set of stress-strain points past the initial yield point.

If the elastic stress exceeds the yield limit σ_y , the following scalar nonlinear equation could be solved:

$$\bar{f}(\Delta\gamma) = q_{n+1}^{trial} - 3G\Delta\gamma - \sigma_y(\bar{\varepsilon}_n^p + \Delta\gamma) \tag{5.3}$$

where q_{n+1}^{trial} is the trial von Mises stress at the increment t_{n+1}, G is the shear modulus, $\Delta\gamma$ is the unknown, σ_y is the yield stress, $\bar{\varepsilon}_n^p$ is the isotropic hardening parameter at the increment t_n and f is the von Mises yield locus, expressed as:

$$f = q(\boldsymbol{\sigma}) - \sigma_y(\bar{\varepsilon}_p) \tag{5.4}$$

where

$$q(\boldsymbol{\sigma}) = \sqrt{\tfrac{1}{2}[(\sigma_{xx} - \sigma_{yy})^2 + (\sigma_{yy} - \sigma_{zz})^2 + (\sigma_{zz} - \sigma_{xx})^2 + 6(\sigma_{xy}^2 + \sigma_{xz}^2 + \sigma_{yz}^2)]} \tag{5.5}$$

Eq. (5.3) is solved using Newton-Raphson method and, with solution $\Delta\gamma$ at hand, the stress and strain are updated:

$$\begin{aligned}
\mathbf{S}_{n+1} &= \mathbf{S}_{n+1}^{trial}\left[1 - \frac{\Delta\gamma 3G}{q_{n+1}^{trial}}\right] \\
\boldsymbol{\sigma}_{n+1} &= \mathbf{S}_{n+1} + P_n^{trial}\mathbf{I} \\
\boldsymbol{\varepsilon}_{n+1}^e &= \frac{1}{2G}\mathbf{S}_{n+1} + \frac{1}{3}\boldsymbol{\varepsilon}_v^{e\ trial}\mathbf{I} \\
\bar{\varepsilon}_{n+1}^p &= \bar{\varepsilon}_n^p + \Delta\gamma
\end{aligned} \tag{5.6}$$

where $P_n^{trial}\mathbf{I}$ is the volumetric stress at increment t_n, and $\frac{1}{3}\boldsymbol{\varepsilon}_v^{e\ trial}\mathbf{I}$ is the volumetric component of the elastic trial strain. Interested readers are referred to [41, 185] for more details on the method of implementation.

Comment 1.3

A final chapter about conclusions and perspectives of this thesis work is missing. For example, is it possible to consider plates with stiffeners as those studied in Chapter 4?

Reply 1.3

The author thank the Reviewer for the useful comment. According to this comment, the Chapter 9 is added to the end of thesis:

Chapter 9

Conclusions and perspectives

9.1 Summary

The dissertation has been focused on the refined structural and nonlinear theories in order to investigate the free vibration and post-buckling response of thin-walled beam and flexible plate structures. In this regard, the CUF has been employed to obtain nonlinear governing equations of the finite beam and plate elements. Then, various assessments have been conducted related to the thin-walled beam and flexible plate structures. The free vibration response of thin-walled isotropic and composite beams has been accurately evaluated, and the Vibration Correlation Technique has been used in order to investigate the variations of natural frequencies in thin-walled laminated isotropic and composite beam structures under compression. The physically and geometrically nonlinear analysis of thin-walled beams has been investigated using Newton–Raphson linearization scheme with the path-following method based on the arc-length constraint. The large-deflection and post-buckling of isotropic and composite plates under axial, in-plane shear and combined loadings considering different strain-displacement assumptions has been analyzed, and the corresponding equilibrium curves and stress distributions have been presented. Furthermore, the effects of stiffeners and displacement boundary conditions in the post-buckled laminated composite plates have been studied. The results have shown that the present method based on the CUF can be efficiently used for accurate structural analysis, including the free vibration and post-buckling of the thin-walled beam and flexible plate structures.

9.2 Concluding remarks

In Chapters 1 and 2, the details of implementation of the CUF framework, and the nonlinear governing equations have been provided. In Chapter 3, higher-order vibration modes in a series of open-section thin-walled beams have been investigated as benchmark problems. Detailed comparisons have been made between the classical beam theories, refined ones based on the CUF, shell models obtained using commercial FE software, and data from the literature. It has been shown that the natural frequencies and mode shapes found using the suggested efficient framework correlate well with those obtained using shell models, which require significantly more computational efforts. The importance of developing models capable of detecting cross-sectional deformations has been demonstrated. The MAC has been successfully used to compare the free vibration modes obtained by various structural theories, and it has been suggested that additional refinement is required for the TE when applied to the complicated cross-section geometries. It has been shown that the selected structural theory has a greater influence in higher-order modes.

In Chapter 4, the vibrations and buckling of thin-walled isotropic and composite beams under compression with different open cross-sections has been evaluated. The effects of axial loads on the variations of the beam structure's natural frequencies have been assessed. The MAC analysis has revealed that the number of related modes for classical models such as Taylor order 1 is much less than that for other Lagrange models. Indeed, classical beam theories eliminate a large number of modes in favor of never-existing rigid cross-section modes. As long as the initial buckling and vibration modes are similar; the VCT may be used to estimate buckling loads based on the decrease in the natural frequencies of the beam under progressive compressive loads. The advantages of the CUF 1D method with efficient LE have been shown for a more complex structural problem involving a channel-shaped composite beam subjected to compression with different number of transverse stiffeners. It been demonstrated that adding transverse stiffeners alters the mode shapes and natural frequencies of the beam structure significantly.

In Chapter 5, the CUF 1D model in combination with a Newton–Raphson linearization scheme based on the path-following method with arc-length constraint has been used to solve physically and geometrically nonlinear beam problems. Numerical results have been presented for square, channel-shaped, and T-shaped beam structures with elastic and elastoplastic materials subjected to large deformations and rotations. It has been demonstrated that for the beams with different cross-sections, the equilibrium curves obtained by CUF 1D elastic and elastoplastic LE models match well with the results of available literature and 3D solid models. The stress distributions have been investigated based on the different LE models, and the results have been compared with 3D FE models. For the elastoplastic material, the plastic zones have been initiated near the top and bottom surfaces of the beam near the clamped edge, where the values of equivalent plastic strain have been increased due to the larger load factor values. Although the DOF and the computational costs of the problems have been reduced significantly using the current method, it can predict the equilibrium curves and the stress distributions of the structure accurately and precisely.

In Chapter 6, it has been shown that the CUF and layer-wise approaches may be used to investigate the large-deflection and post-buckling of rectangular isotropic and composite plates.The well-known von Kármán theory for nonlinear deformations of plates has been evaluated with several modifications. The equilibrium curves and stress distributions for different isotropic and composite plates have been provided and analyzed in detail. Different factors influencing the nonlinear response of plates, including the stacking sequence, number of layers, loading and edge conditions, have been thoroughly studied. In comparison with the von Kármán theory and its modifications, the full nonlinear model has been proved to be more reliable in order to investigate the correct equilibrium curves and stress distributions in the very large displacements and far post-buckling regime. It has been indicated that the buckling strength of the composite plates with clamped edge conditions is greater than those of the composite plates with other studied edge conditions, and the presence of a free edge, considerably reduces the buckling strength of the plate structures.

In Chapter 7, the stiffeners and boundary conditions effects on the geometrically nonlinear response of laminated composite plates under various strain-displacement assumptions have been studied. It has been demonstrated that the stiffeners' material properties have a significant impact on the nonlinear post-buckling behaviors, and the presence of stiffeners limits the rotations at the loaded edges of the plate structure by enforcing uniform edge displacement. Lower values of the stiffener's material properties have resulted in a post-buckling behavior that is similar to the response of the plate in the absence of the stiffener. On the other hand, higher values of material properties for the stiffener have resulted in rotational limitations in the loaded edges. Lamination angles and stacking sequence have shown to be important in the composite plate structure's buckling and post-buckling behaviors. It has been shown that the quadratic shear stress distributions can be predicted with high accuracy using the cubic LD3 CUF plate models. The nonlinear response of the composite plate above the limit load and snap-through instability has been predicted using the presented CUF plate model.

In Chapter 8, a modeling technique based on the CUF, layer-wise theory, and full Green–Lagrange nonlinear relations has been proposed in order to model the real shear conditions, and investigate the nonlinear response of composite plates subjected to shear and combined loadings. It has been indicated that for both Baron Epoxy and Carbon Epoxy composite plates with different lamination angles and shear loading conditions, the results obtained by the presented CUF-based method match well with the results reported in the available literature. It has been demonstrated that the direction of applied shear plays an important role in the geometrically nonlinear response of angle-ply composite plates. As a result, the plates under negative shear show higher buckling strength. Biaxial compressive loading has resulted in the decrease of buckling strength and the rigidity of structure because of the intensification effects on the induced deflections by the shear loading. Nonetheless, biaxial tensile loading has resulted higher load-carrying capacity of the plate structure.

9.3 Future directions

Due to the reliable and accurate results of the CUF in solving geometrically and physically nonlinear problems of structures, further developments of the proposed methodology could be focused on a nonlinear local analysis and a localized buckling with the advantage of coupling the global/local approach with optimization tools to reduce computation time. Furthermore, the same nonlinear methodology will also be adopted to perform dynamic analyses. Other important topics that could be further developed could be the extension of CUF-based nonlinear finite elements for the analysis of deployable space structures, elastomers and mechanical meta-materials. Furthermore, Hyperelastic models could be implemented in the CUF 1D or CUF 2D frameworks in order to be used in the complex materials such as biological soft tissues and organs. For instance, the soft materials are susceptible to the occurrence of instability and failure that needs to be accurately predicted; therefore, using the

CUF, the constitutive relations of soft tissues or complex structures using continuum approaches could be investigated, and in-depth study on the material behavior of soft matters could be presented. In addition, future extensions could be focused on high-velocity impact problems and progressive failure of composite structures. Also, the effects of transverse stiffeners nonlinearities on the dynamic response of the beam and plate structures under compression deserve special attention.

Also, the author would like to thank the Reviewer for the valuable and detailed comments in the PDF file. All the comments in the file have been addressed accordingly, and the typos have been corrected. Some points which needed further clarifications from the PDF file are provided in the following:

Comment 1.4

What is the length of the beam? P 70.

Reply 1.4

The length of the beam is 670 mm. This has been added in the explanations of the figure.

Comment 1.5

Could you provide a DOF comparison with ABQ? P 101.

Reply 1.5

Table 4.35 with the DOF comparison of box, I-shaped, and channel-shaped beams has been added to the revised version:

Table 4.35 The comparison of ABQ shell and CUF 1D models employed for the investigated beam structures

Model	DOF	Number of elements	Element type
ABQ shell-box beam	32832	1800	Quadratic S8R
ABQ shell-I-shaped bam	26748	1400	Quadratic S8R
ABQ shell-Channel-shaped beam	28572	1500	Quadratic S8R
CUF 1D-LE-box beam	18117	20B4	4-node beam
CUF 1D-LE-I-shaped bam	17019	20B4	4-node beam
CUF 1D-LE-Channel-shaped beam	15921	20B4	4-node beam

Comment 1.6

Could you provide a figure of the geometry in this case? P 105.

Reply 1.6

The author is grateful for the suggestion. The relevant figure has been added:

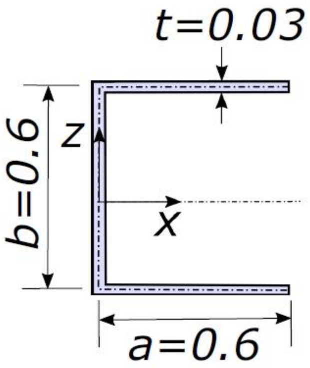

Fig. 4.22 Geometry of thin-walled channel-shaped composite beam (dimensions in mm)

Comment 1.7

Please, provide the von Mises constitutive model. P 129.

Reply 1.7

Some details of von Mises constitutive model is added to the revised version, and are also provided in Reply 1.2.

Comment 1.8

Which model do you identify with the prefix 1? P 136.
What does it mean the prefix 2? P 143

Reply 1.8

The author thank the Reviewer for pointing this out. The prefix 1 before the acronym LD is excessive, and is removed in the updated version. Some prefixes before LD are used in Fig. 6.5, which refer to the number of elements in the thickness direction of plate structure. In fact, the aim is to assess the effects of elements in the thickness direction of plate on the distribution of transverse shear stress. The relevant explanation is also added to the text of updated version.

can accurately describe the quadratic shear stress distribution. Note that the prefixes before LD in this figure refer to the number of elements in the thickness direction of plate structure.

Comment 1.9

According to which convention is it negative? Please, explain. P 193.

Reply 1.9

The author is grateful for this comment. A schematic figure of negative shear loading along with the relevant literature is shown in the Fig. 6.27:

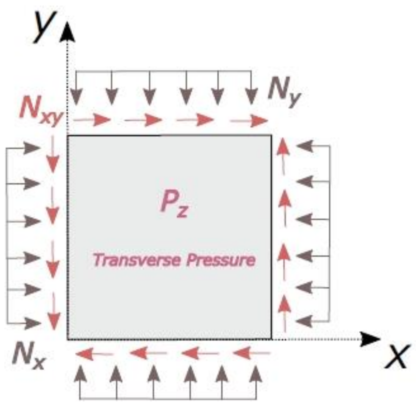

Fig. 6.27 Combined loading of a laminated composite plate: negative in-plane shear, in-plane compression, and the uniform transverse pressure [240]

Doctoral Examination Committee 2, Professor Bagassi:

This thesis presents refined nonlinear structural theories for the free vibration and post-buckling response of thin-walled beam and flexible plate structures. In this regard, the Unified Formulation is employed to obtain nonlinear governing equations of the finite beam and plate elements. Then, various assessments are conducted related to the thin-walled beam and flexible plate structures. The free vibration response of thin-walled isotropic and composite beams is accurately evaluated, and the Vibration Correlation Technique is used in order to investigate the variations of natural frequencies in thin-walled laminated isotropic and composite beam structures under compression. The physically and geometrically nonlinear analysis of thin-walled beams is also investigated using Newton–Raphson linearization scheme with the path-following method based on the arc-length constraint. The large-deflection and post-buckling of isotropic and composite plates under axial, in-plane shear and combined loadings are analyzed considering different strain-displacement assumptions, and the corresponding equilibrium curves and stress distributions are presented. Furthermore, the effects of load and displacement boundary conditions in the post-buckled laminated composite plates are investigated, and the effects of stiffeners are assessed. The results show that the present method based on the Unified Formulation can be efficiently used for accurate structural analysis, including the free vibration and post-buckling of the thin-walled beam and flexible plate structures.

The manuscript is well written and its structure is satisfactory. Each section is well organized and properly introduced and developed. Figures, Tables and related captions are well finished and the bibliography is complete.

The general view about the thesis is very positive, however minor revisions are needed in order to clarify the following points and to fix a few typos.

Comment 2.1

In sections 3, 4, 5, and 6 conclusions the author claims the reduction of DoF caused by the use of the CUF approach. A table with the DoF comparison between the CUF, the ABQ and the literature model could be very useful for the reader (there is one in section 5 for example).

Reply 2.1

The author thank the Reviewer for the useful comment. According to the comment of Reviewer, some tables have been added to the previous tables. In the revised version, the tables in Chapters 3-6 including the DOF comparison of ABQ and CUF models are as follows:

Table 3.11 The details of ABQ shell and CUF 1D models employed for the cruciform beam

Model	DOF	Number of elements	Element type	Section discretization	Time (Sec)
ABQ shell-coarse	6342	320	Quadratic S8R	8	25.16
ABQ shell-medium	24198	1280	Quadratic S8R	16	31.47
ABQ shell-fine	94470	5120	Quadratic S8R	32	53.89
CUF 1D-LE	2736	5B4	4-node beam	9L9	4.33
CUF 1D-LE	9765	10B4	4-node beam	17L9	11.48
CUF 1D-LE	27999	20B4	4-node beam	25L9	35.35

Table 3.29 The comparison of ABQ shell and CUF 1D models employed for the investigated beam structures

Model	DOF	Number of elements	Element type	Section discretization
ABQ shell-beam1	27102	1440	Quadratic S8R	18
ABQ shell-beam2	28554	1520	Quadratic S8R	19
ABQ shell-beam3	64854	3520	Quadratic S8R	42
ABQ shell-beam4	60498	3280	Quadratic S8R	41
CUF 1D-LE-beam1	15921	20B4	4-node beam	14L9
CUF 1D-LE-beam2	17019	20B4	4-node beam	15L9
CUF 1D-LE-beam3	18117	20B4	4-node beam	16L9
CUF 1D-LE-beam4	19215	20B4	4-node beam	17L9

Table 4.10 The first nine natural frequencies of the unloaded thin cruciform beam based on the CUF 1D Lagrange model and the thin ABQ shell model

				Natural Frequency (Hz)								
Model	Number of elements	Lag. Points	DOF	Mode 1	Mode 2	Mode 3	Mode 4	Mode 5	Mode 6	Mode 7	Mode 8	Mode 9
CUF 1D (Lag.)	20 B4	105	19215	32.17	64.46	96.98	129.84	163.17	197.06	231.64	250.00	256.39
Thin ABQ shell	1680 S8R	-	52396	30.82	61.76	92.93	124.47	156.47	189.05	222.32	254.71	261.08

Table 4.35 The comparison of ABQ shell and CUF 1D models employed for the investigated beam structures

Model	DOF	Number of elements	Element type
ABQ shell-box beam	32832	1800	Quadratic S8R
ABQ shell-I-shaped bam	26748	1400	Quadratic S8R
ABQ shell-Channel-shaped beam	28572	1500	Quadratic S8R
CUF 1D-LE-box beam	18117	20B4	4-node beam
CUF 1D-LE-I-shaped bam	17019	20B4	4-node beam
CUF 1D-LE-Channel-shaped beam	15921	20B4	4-node beam

Table 5.2 Computational size of the investigated models for the square beam

Model	DOF	Computational time (s)
ABQ-3D Coarse	1869	83
ABQ-3D Medium	11001	194
ABQ-3D Refined	44085	546
CUF 1D (LE-4L9)	4575	56
CUF 1D (LE-9L9)	8967	101
CUF 1D (LE-16L9)	14823	171
CUF 1D (TE: N=1)	549	138
CUF 1D (TE: N=2)	1098	483
CUF 1D (TE: N=3)	1830	2125

Table 5.5 Computational size of the investigated models for the C-shaped beam

Model	DOF	Computational time (s)
ABQ-3D Coarse	9867	419
ABQ-3D Medium	125814	1193
ABQ-3D Refined	245049	2911
CUF 1D (LE-5L9)	6039	322
CUF 1D (LE-8L9)	9333	421
CUF 1D (LE-13L9)	14823	730

Table 5.8 Computational size of the investigated models for the T-shaped beam

Model	DOF	Computational time (s)
ABQ-3D Coarse	9393	241
ABQ-3D Medium	18453	477
ABQ-3D Refined	60549	1459
CUF 1D (LE-5L9)	6039	142
CUF 1D (LE-7L9)	8235	364
CUF 1D (LE-9L9)	10431	484

Table 6.11 The comparison of displacement values at the fixed load of $\frac{N_x ba}{E_2 h^3} = 300$ and the normalized linear buckling loads for a cross-ply $[0/90]_2$ laminate

Model	DOF	u_z (mm)	Linear Buckling Load (N/m)
CUF 2D Full NL 20×5Q9-LD1	6765	1.422	503360
ABQ 2D NL 60×15 S8R	17106	1.134	497658
ABQ 3D NL 60×15×4 C3D20R	24993	1.428	498976

Comment 2.2

p. 4-5 please define the tau index. Is it the cross-section index?

Reply 2.2

The author thank the Reviewer for pointing this out. In the CUF framework, theories of beam structures are defined through the definition of cross-section expansion function $F_\tau(x,z)$, where τ is expansion function index, and varies from 1 to N. Also, it should be noted that N refers to the number of polynomial terms in the cross-section expansion function. The relevant explanation has been also added to the revised version.

Comment 2.3

p. 5 clarify if the Ni functions depend on tau

Reply 2.3

The author is thankful to the Reviewer. $N_i(y)$ refers to 1D shape functions related to the i^{th} node along the beam axis in y direction. The choice of the axial shape functions N_i is independent of the choice of the cross-sectional expansion functions F_τ , leading to significant flexibility in the structural modelling. The relevant explanation has been also added to the revised version.

Comment 2.4

p. 13 I think after eq. 2.6, "lambda" has to be symbolic char (probably in latex the \ is missing)

Reply 2.4

The Reviewer is right on that. The mentioned typo is corrected in the revised version.

Comment 2.5

p. 36 the author shall clarify why he chooses two arbitrary cross sections. The author considers all beam clamped, did the author analyse or take in account the effects of different BCs on the convergence and validation study?

Reply 2.5

The author thank the Reviewer for pointing this out. The thin-walled open cross-section beams and the mentioned arbitrary cross-section are selected based on the benchmark beam problems introduced by Chen [88], which has been introduced in Section 3.2. The aim has been providing standard beam examples and providing benchmark reference solution for them. Regarding the point about boundary conditions effect on the convergence analysis, the author agree with the Reviewer that the convergence study could be very problem dependent. This effect has been considered, and for the sake of brevity, in Chapter 3, the convergence study for the clamped-free edge conditions has been provided in Section 3.3 of the thesis due to the fact that the main assessments of the chapter have been focused on this boundary conditions.

Comment 2.6

p. 47 deviations between the experiments and the CUF are low, but still around the 4-5%, the author shall elaborate about the reasons behind those deviations (same comment applies to differences between ABQ and the CUF).

Reply 2.6

The author thank the Reviewer for this concern. In fact, many factors could result in such deviation. For example, there are different environmental, human, and equipment parameters that could play role during the extraction of data in different steps of the experimental approach, as in Ref [97], the natural frequencies of the beam have been obtained exciting the specimen by means of several impulses provided by a non-instrumented hammer and detecting the frequencies using the Peak Picking technique using the PZT pickups or Laser sensors. Furthermore, in the computational method, the approximation introduced by the kinematics of the problem or FEM analysis could lead to such low deviations. Accordingly, the ABQ and CUF models employ different FEM formulations, and are based on different structural theories of shells and beam structures. The relevant explanation has been also added to the revised version.

> match well with experimental results. Note that small deviations of less than 6.5% could be due to many factors influencing different steps of experimental approach during the frequency extraction process, or the approximations introduced by the kinematics assumption or FEM method. Accordingly, the ABQ and CUF models employ different FEM formulations, and are based on different structural theories of shells and beam structures.

Comment 2.7

p. 79 "As can be seen in Table" the number of the table is missing.

Reply 2.7

The Reviewer is right on that, the mentioned point is corrected in the revised version.

Comment 2.8

p. 96 The author states that the differences between the theories are more significant for the higher order. Further elaboration would be appreciated.

Reply 2.8

The author is grateful for the suggestion. In Fig. 4.17, the three modes of CUF 1D model match well with ABQ shell models. Although for results of Ref. [155], the same agreement is seen for the first two modes, the third mode shows a small deviation with CUF and ABQ models. Different factors could result in such deviation, and one possibility could be due to the fact that, when dealing with higher modes, the effects of employing different beam structural theories become more visible (as highlighted in Chapter 3). In fact, many structural models could miss some of the cross-sectional deformations that results in the stiffer structure and higher approximation of natural frequency. The relevant explanation has been also added to the revised version.

shell and the literature. In these graphs, for the third mode of Ref. [155], which employs higher-order beam theories, some discrepancies with the CUF and ABQ shell results can be seen. This could be explained by the fact that the difference between different structural theories becomes more important in higher modes. In fact, many structural models could miss some of the cross-sectional deformations that results in the stiffer structure and higher approximation of natural frequency. The suggested CUF 1D approach, on the other hand, is efficient in higher-order modes and corresponds well with the ABQ shell findings.

Comment 2.9

P.98 fix the typo "thin0walled"

Reply 2.9

The mentioned typo is corrected in the revised version.

Comment 2.10

p. 108 Further elaboration about the physical explanation of these results would be appreciated.

Reply 2.10

The author thank the Reviewer for pointing this out. A relevant explanation has been added to the revised version:

Additionally, Table 4.38 illustrates the beam's first three mode shapes. As can be seen in the mode shapes of this figure, the localized deformation along the length of the beam are decreased as the number of stiffeners are increased. In fact, the presence of stiffeners imposes some limitations for the localized deformations along the beam that leads to the increase of buckling strength and natural frequency. For instance, as will be further discussed in the following, the second and third modes of the case with five stiffeners show highest buckling loads and natural frequencies.

Furthermore, some explanations on the mentioned mode shapes have been provided for Fig. 4.23 and 4.24.

Fig. 4.24 compares beams with three and five stiffeners. These figures illustrate how the number of transverse stiffeners affects the buckling behavior and natural frequencies of this beam structure. The third mode of the case with five stiffeners has the highest natural frequency. It is worth mentioning that adding stiffeners alters the mode shapes and natural frequencies of the beam structure remarkably. As a result, a mode-by-mode comparison may not be possible for the models with different number of stiffeners. As seen in Fig. 4.23, the third mode of the model with one stiffener has the highest natural frequency in the unloaded condition. However, it has a substantially lower buckling strength than the second mode of the beam without stiffener. Also, other examples from Fig. 4.24 could be the second and third modes of the beam with five stiffeners, with the former exhibiting the highest buckling strength and the latter exhibiting the highest natural frequency in the unloaded state.

Comment 2.11

P.136 please clarify what 1LD2 refers to (prefix 1 is not clear).
P.143 please clarify what 2LD3 refers to (prefix 2 is not clear).

Reply 2.11

The author agree with the Reviewer. The prefix 1 before the acronym LD is excessive, and is removed in the updated version. Some prefixes before LD are used in Fig. 6.5, which refer to the number of elements in the thickness direction of plate structure. In fact, the aim is to assess the effects of elements in the thickness direction of plate on the distribution of transverse shear stress. The relevant explanation is also added to the text of updated version.

can accurately describe the quadratic shear stress distribution. Note that the prefixes before LD in this figure refer to the number of elements in the thickness direction of plate structure.

Comment 2.12

P.167 fix the typo "K'arm'a'n" (Latex)

Reply 2.12

The mentioned typo is corrected in the revised version.

Comment 2.13

A final "conclusions and future work" chapter shall be added at the end of the manuscript.

Reply 2.13

The author thank the Reviewer for the useful comment. According to this comment, the Chapter 9 is added to the end of thesis:

Chapter 9

Conclusions and perspectives

9.1 Summary

The dissertation has been focused on the refined structural and nonlinear theories in order to investigate the free vibration and post-buckling response of thin-walled beam and flexible plate structures. In this regard, the CUF has been employed to obtain nonlinear governing equations of the finite beam and plate elements. Then, various assessments have been conducted related to the thin-walled beam and flexible plate structures. The free vibration response of thin-walled isotropic and composite beams has been accurately evaluated, and the Vibration Correlation Technique has been used in order to investigate the variations of natural frequencies in thin-walled laminated isotropic and composite beam structures under compression. The physically and geometrically nonlinear analysis of thin-walled beams has been investigated using Newton–Raphson linearization scheme with the path-following method based on the arc-length constraint. The large-deflection and post-buckling of isotropic and composite plates under axial, in-plane shear and combined loadings considering different strain-displacement assumptions has been analyzed, and the corresponding equilibrium curves and stress distributions have been presented. Furthermore, the effects of stiffeners and displacement boundary conditions in the post-buckled laminated composite plates have been studied. The results have shown that the present method based on the CUF can be efficiently used for accurate structural analysis, including the free vibration and post-buckling of the thin-walled beam and flexible plate structures.

9.2 Concluding remarks

In Chapters 1 and 2, the details of implementation of the CUF framework, and the nonlinear governing equations have been provided. In Chapter 3, higher-order vibration modes in a series of open-section thin-walled beams have been investigated as benchmark problems. Detailed comparisons have been made between the classical beam theories, refined ones based on the CUF, shell models obtained using commercial FE software, and data from the literature. It has been shown that the natural frequencies and mode shapes found using the suggested efficient framework correlate well with those obtained using shell models, which require significantly more computational efforts. The importance of developing models capable of detecting cross-sectional deformations has been demonstrated. The MAC has been successfully used to compare the free vibration modes obtained by various structural theories, and it has been suggested that additional refinement is required for the TE when applied to the complicated cross-section geometries. It has been shown that the selected structural theory has a greater influence in higher-order modes.

In Chapter 4, the vibrations and buckling of thin-walled isotropic and composite beams under compression with different open cross-sections has been evaluated. The effects of axial loads on the variations of the beam structure's natural frequencies have been assessed. The MAC analysis has revealed that the number of related modes for classical models such as Taylor order 1 is much less than that for other Lagrange models. Indeed, classical beam theories eliminate a large number of modes in favor of never-existing rigid cross-section modes. As long as the initial buckling and vibration modes are similar; the VCT may be used to estimate buckling loads based on the decrease in the natural frequencies of the beam under progressive compressive loads. The advantages of the CUF 1D method with efficient LE have been shown for a more complex structural problem involving a channel-shaped composite beam subjected to compression with different number of transverse stiffeners. It been demonstrated that adding transverse stiffeners alters the mode shapes and natural frequencies of the beam structure significantly.

In Chapter 5, the CUF 1D model in combination with a Newton–Raphson linearization scheme based on the path-following method with arc-length constraint has been used to solve physically and geometrically nonlinear beam problems. Numerical results have been presented for square, channel-shaped, and T-shaped beam structures with elastic and elastoplastic materials subjected to large deformations and rotations. It has been demonstrated that for the beams with different cross-sections, the equilibrium curves obtained by CUF 1D elastic and elastoplastic LE models match well with the results of available literature and 3D solid models. The stress distributions have been investigated based on the different LE models, and the results have been compared with 3D FE models. For the elastoplastic material, the plastic zones have been initiated near the top and bottom surfaces of the beam near the clamped edge, where the values of equivalent plastic strain have been increased due to the larger load factor values. Although the DOF and the computational costs of the problems have been reduced significantly using the current method, it can predict the equilibrium curves and the stress distributions of the structure accurately and precisely.

In Chapter 6, it has been shown that the CUF and layer-wise approaches may be used to investigate the large-deflection and post-buckling of rectangular isotropic and composite plates.The well-known von Kármán theory for nonlinear deformations of plates has been evaluated with several modifications. The equilibrium curves and stress distributions for different isotropic and composite plates have been provided and analyzed in detail. Different factors influencing the nonlinear response of plates, including the stacking sequence, number of layers, loading and edge conditions, have been thoroughly studied. In comparison with the von Kármán theory and its modifications, the full nonlinear model has been proved to be more reliable in order to investigate the correct equilibrium curves and stress distributions in the very large displacements and far post-buckling regime. It has been indicated that the buckling strength of the composite plates with clamped edge conditions is greater than those of the composite plates with other studied edge conditions, and the presence of a free edge, considerably reduces the buckling strength of the plate structures.

In Chapter 7, the stiffeners and boundary conditions effects on the geometrically nonlinear response of laminated composite plates under various strain-displacement assumptions have been studied. It has been demonstrated that the stiffeners' material properties have a significant impact on the nonlinear post-buckling behaviors, and the presence of stiffeners limits the rotations at the loaded edges of the plate structure by enforcing uniform edge displacement. Lower values of the stiffener's material properties have resulted in a post-buckling behavior that is similar to the response of the plate in the absence of the stiffener. On the other hand, higher values of material properties for the stiffener have resulted in rotational limitations in the loaded edges. Lamination angles and stacking sequence have shown to be important in the composite plate structure's buckling and post-buckling behaviors. It has been shown that the quadratic shear stress distributions can be predicted with high accuracy using the cubic LD3 CUF plate models. The nonlinear response of the composite plate above the limit load and snap-through instability has been predicted using the presented CUF plate model.

In Chapter 8, a modeling technique based on the CUF, layer-wise theory, and full Green–Lagrange nonlinear relations has been proposed in order to model the real shear conditions, and investigate the nonlinear response of composite plates subjected to shear and combined loadings. It has been indicated that for both Baron Epoxy and Carbon Epoxy composite plates with different lamination angles and shear loading conditions, the results obtained by the presented CUF-based method match well with the results reported in the available literature. It has been demonstrated that the direction of applied shear plays an important role in the geometrically nonlinear response of angle-ply composite plates. As a result, the plates under negative shear show higher buckling strength. Biaxial compressive loading has resulted in the decrease of buckling strength and the rigidity of structure because of the intensification effects on the induced deflections by the shear loading. Nonetheless, biaxial tensile loading has resulted higher load-carrying capacity of the plate structure.

9.3 Future directions

Due to the reliable and accurate results of the CUF in solving geometrically and physically nonlinear problems of structures, further developments of the proposed methodology could be focused on a nonlinear local analysis and a localized buckling with the advantage of coupling the global/local approach with optimization tools to reduce computation time. Furthermore, the same nonlinear methodology will also be adopted to perform dynamic analyses. Other important topics that could be further developed could be the extension of CUF-based nonlinear finite elements for the analysis of deployable space structures, elastomers and mechanical meta-materials. Furthermore, Hyperelastic models could be implemented in the CUF 1D or CUF 2D frameworks in order to be used in the complex materials such as biological soft tissues and organs. For instance, the soft materials are susceptible to the occurrence of instability and failure that needs to be accurately predicted; therefore, using the

CUF, the constitutive relations of soft tissues or complex structures using continuum approaches could be investigated, and in-depth study on the material behavior of soft matters could be presented. In addition, future extensions could be focused on high-velocity impact problems and progressive failure of composite structures. Also, the effects of transverse stiffeners nonlinearities on the dynamic response of the beam and plate structures under compression deserve special attention.